Nanotube synthesis from reaction of 4-chloro phenoxy acetate with zinc layered hydroxide

Abbas Matrood Bashi

Objective Intercalations of plant growth regulator 4-chloro phenoxy acetate (4CPA) with zinc oxide (ZnO), developed using ZnO-layered hydroxide (ZLH) as host material and 4CPA as a guest.
Methods Ion exchange technique via sol-gel method synthesized under aqueous environment, resulted in the formation of inorganic–organic nanotube materials.
Results The release of 4CPA from its nanohybrid was found to occur in a controlled manner, governed by pseudo-second order kinetics model. The maximum amount of 4CPA released was governed by pseudo-second order kinetics model. Powder X-ray diffraction showed that the basal spacing of the nanohybrid was developed with the increasing of 4CPA concentrations; the maximum concentration of 0.2M shows an interlayer basal of 1.9 nm. FTIR study showed that the intercalated 4CPA-ZnO spectral feature is generally similar to that of 4CPA, but with bands sightly shifted due to the formation of host–guest nanotubes.
Conclusion The resulted nanotubes were characterized by using scanning electron microscopy (SEM), and transmission electronic microscope (TEM), shows a uniform nanoparticles and monodisperse with average diameter of 35 nm, which correlated a very well with size scale obtained from XRD data. The development of crystals is the function of concentrations.
Keywords zinc oxide, nanomaterials, 4-chloro phenoxy acetic acid, intercalations

Introduction

Zinc oxide (ZnO) has attracted much attention for its wide direct band gap (3.37 eV) and large exciton binding energy (60 meV) at room temperature.[1] Nanoparticles have been widely used in optical, resonant, electrical and magnetic fields. Various chemical methods have been used for the production of nanoparticles with narrow size distribution such as micro emulsion method, electro spray pyrolysis and hydrothermal methods. Semi-conducting and piezoelectric material have many useful properties, such as optical absorption, emission,[2] conductivity,[3] photo catalysis[4] and sensitivity to gases.[5] Therefore, many efforts are concentrated on the synthesis of ZnO materials.[6–13] Among those methods based on physical and solution-based chemical technologies to synthesize ZnO particles, organic complexion additives are always used to control the growth of the crystals.[14–20] By the addition of organic active molecules, Zn complex will be formed, which owns certain stability in both air and aqueous solution. So, it is necessary to find some effective methods to induce the conversion of the Zn complex into ZnO particles. Thermal decomposition is a common method to get ZnO particles. For example, fiber-like ZnO materials from the decomposition of bis(acetylacetonato) zinc fibers at 110°C in the presence of superheated steam was obtained,[19] material scientists are inclined to realize the diversity of morphological ZnO particles with solution-phase method, which is conducted by precipitating the preformed complex into ZnO sediments,[20–22] 4-chloro phenoxyacetic acid (4CPA), as one of the common organic additive. For example, in this work a stable complex composed of 4CPA was formed before further treatments (at 30°C), and then ZnO particle aggregates or rods were obtained. A similar work was reported by Shishido et al.[23] All these results prove that the complex plays an important role as templates, a novel method, which supplies a facile technology to transform the preformed Zn-4CPA complex into ZnO particles with various morphologies, which will be a good prospect for material science. In this work, we have designed a novel route to form templates (Zn-4CPA complex) first, and then induce the hydrolysis of the template to produce ZnO particles. This method has its special advantages: (1) The transformation of Zn-4CPA complex is facile and quite different from those traditional ways like thermal decomposition, refluxing and hydrothermal treating and heating; (2) We select 4CPA as complex reagents to realize the diversity of morphological ZnO particles; and (3) It is an economical route with low energy consumption (low temperature, normal atmospheric pressure). Novel slice-like and quasi sphere-like ZnO particles have been successfully fabricated accordingly. The growth mechanisms of the nanoparticles induced an interaction between the 4CPA and Zn cations.

Materials and Methods

ZnO purchased from ACrose (USA), 4CPA from Merck, was used without further purification. Solutions of 0.05, 0.1, 0.2M of 4CPA were prepared by dissolving in 50 ml of 90% ethanol. This solution was dropped into a solution prepared by 1 gm of ZnO in 100 ml de-ionized water, in a conical flask, the resulted solution under N_2 gas was stirred, and formation of gel suspension started, followed by temperature aging at 70°C for 18 hours. It was then cooled, centrifuged and washed four times with de-ionized water, dried in oven at 70°C Then it was grinded and kept in a sample bottle for further analyses.

Characterizations

Powder X-ray diffraction (PXRD) patterns were obtained with a Shimadzu XRD-6000 powder diffractometer using λ = 1.540562 Å at 40 kV and 30 mA with a scan rate of 0.5 min/degrees. Fourier transform infrared (FTIR) spectra were recorded by using a spectrophotometer thermo Nicolet Ft-IR Nexus self supporting sample in the range of 4000–400 cm^{-1},

Department of Clinical Laboratories, University of Karbala-Iraq, Karbala, Iraq.
Correspondence to Abbas Matrood Bashi (email: abbasmatrood493@gmail.com).
(*Submitted: August 2014 – Revised version received: 20 January 2015 – Accepted: 28 January 2015 – Published online: Spring 2015*)

and the thermogravimetry, derivative thermogravimetry (TG/DTG) were carried out with a Setaram TG-DSC-11 apparatus with fully programmable heating and cooling sequence sweep gas valve switching and data analysis. The surface morphology and bulk structure of the sample was observed by scanning electron microscope (SEM) model JOEL (JSM-6400) and TEM Hitachi (H 7100).

Results and Discussion

The evidence for phase structure of the as-prepared sample was obtained by XRD pattern, as shown in Fig. 1. All the diffraction peaks can be indexed to those of hexagonal ZnO. After refinement, the lattice constants, a = 3.251 Å, c = 5.210 Å were obtained, which was very close to the reported value for ZnO (a = 3.253 Å, c = 5.209, JCPDS card, No. 80-0075). The broadening of the ZnO XRD peaks suggests that the grain sizes are on a nanometer scale. The average particles size was estimated to be 70 nm based on the Scherrer equation, D ¼ Kλ βdcosθ; here K is shape factor of average crystallite, λ is wavelength for the Kα1 (1.54056 Å), β is full width at half-maximum of the diffraction line and θ is Bragg's angle. Fig. 1 shows that the XRD patterns of the synthesized nanosheet thin films made up of nanorods progressing with the intensities of the ray (003) clearly was concentration dependent; and within the same time this sharp peak moved in the direction of small angle, which indicates that good crystals were made from the resulted 4CPA-ZnO when we used high concentration from 4CPA.

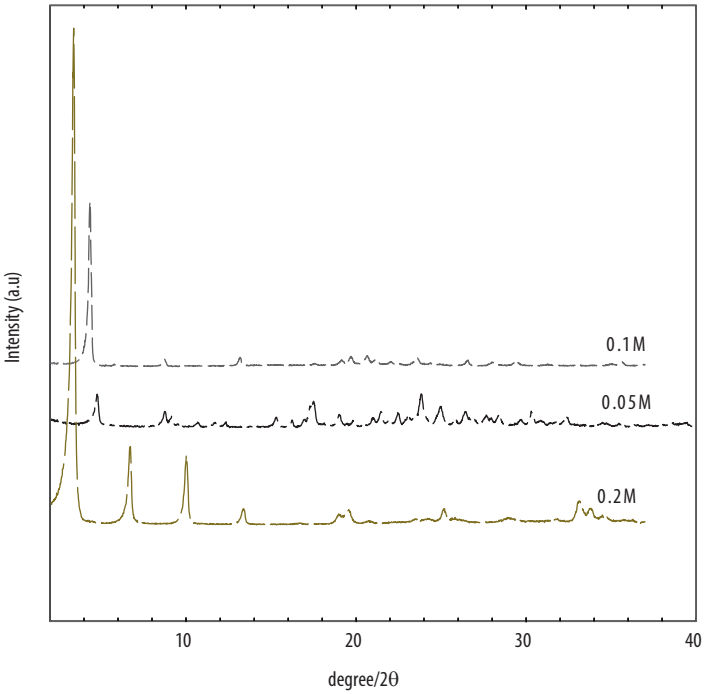

Fig. 1 **XRD pattern of three concentrations of 4CPA intercalated with ZnO nanohybrids.**

It is clear that the samples are indexed to typical wurtzite-type ZnO. And all the sharp diffraction peaks indicate good crystals of the obtained nanostructures up to 0.2M concentrations of 4CPA, the corresponding energy-dispersive spectra were recorded. It can be obviously observed that the spectra of sample as-grown and the EDS studies (Fig. 3) reveal that no trace of other elements was detected in any grown samples. These XRD patterns and EDS spectra confirm the formation of pure ZnO intercalated with 4CPA to form a nanomaterial. The morphology of the as-prepared sample was investigated by SEM. Fig. 2 shows a typical SEM image of the ZnO–WPI (whey protein isolate) composite.

Table 1 shows the EDS studies of ZnO intercalated with 4CPA in three positions as we have seen in Fig. 2, the elements composite of the ZnO with 4CPA-nanosheet.

From this TEM micrograph, it is clear that our product is a composite of ZnO and WPI, i.e. WPI granule with a size of about 70 nm embedded with several ZnO nanoparticles. These nanoparticles are uniform and monodisperse with average diameter of 35 nm, which correlates very well with size scale obtained from XRD data (70 nm). The development of crystals is function of concentrations as we see in Fig. 1 up to the concentration of 0.2M which is

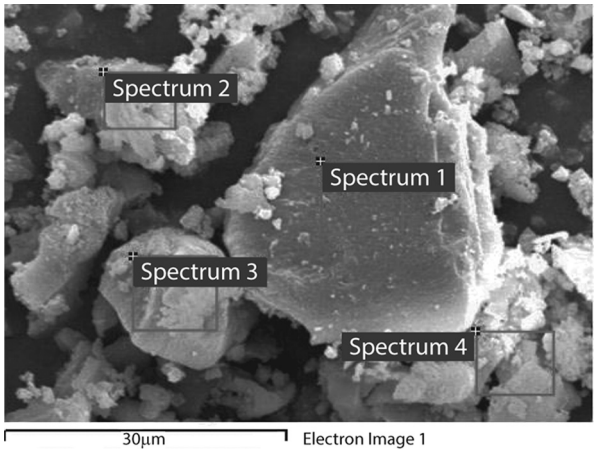

Fig. 2 **A typical SEM image of the ZnO–WPI composite processing option: All elements were analyzed (normalized).**

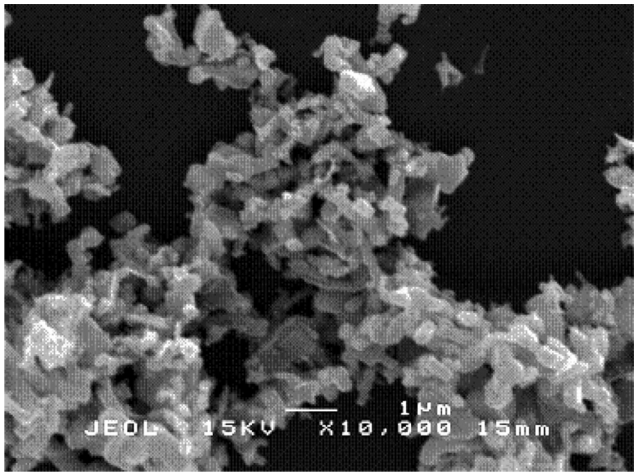

Fig. 3 **SEM image of hexagonal crystals.**

reported to be 1.95 nm for the 003 plane. The ZnO–WPI particles were stable under the electron beam in vacuum used for TEM measurements, suggesting that the binding between ZnO and WPI is strong. The corresponding selected area electron diffraction (SAED) pattern of ZnO nanoparticle is shown as an inset in Fig. 3 as a hexagonal crystal structure.

Figs. 6 and 7 show the TG-DTG curves of ZnO, and ZnO-4CPA shows the details of the TG, which reveal two distinguishable weight loss steps. The first step indicate losses 9.67% started from 37°C terminating at 143°C with maximum temperature of 138.7°C; this is attributed to the loss of physical adsorbed and the interlayer water. The next stage with total loss which is equal to 35.3% at the temperature between 250–396°C and the maximum at 320°C, is due to the decomposition and subtle combustion of 4CPA. The total loss achieved is around 47.3%. This is in accord with the elemental analysis.

D_3h symmetry is confirmed by the presence of band at 834 cm^{-1} (Fig. 8).[13] The OH vibrations of the layers can be observed by a band in the 3600–3000 cm^{-1} region. This band has a broad base due to hydrogen bonds established with the hydration water molecules.

The FTIR spectrum of the hybrid presented C–H vibrations of the organic chain at 2932 cm^{-1} and the asymmetric and symmetric stretching of COO– appears at 1550 and 1410 cm^{-1}. The latter band is overlapped with C–H vibrations, which forms a shoulder at 1450 cm^{-1} (Fig. 8).

Table 1. **EDX elements analysis**

Spectrum	C	O	Cl	Zn	Total
Spectrum 1	45.15	15.98	15.76	23.11	100.00
Spectrum 2	41.78	14.49	14.98	22.93	100.00
Spectrum 3	47.71	14.71	12.82	23.97	100.00
Max.	47.71	14.49	18.76	23.97	
Min.	41.78	13.98	12.82	22.93	

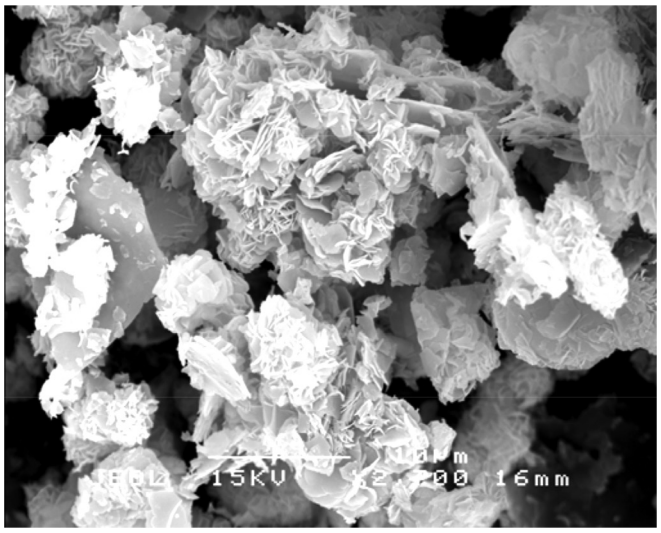

Fig. 4 **SEM image shows the superficial interactions between ZnO layers and the anion 4CPA.**

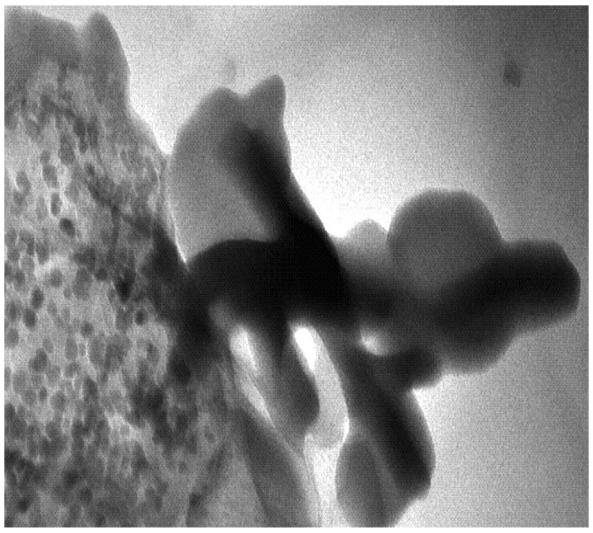

Fig. 5 **Transmitting Electronic Microscope (TEM) shows the nanotube of the resulted nano composite from 4CPA and ZnO.**

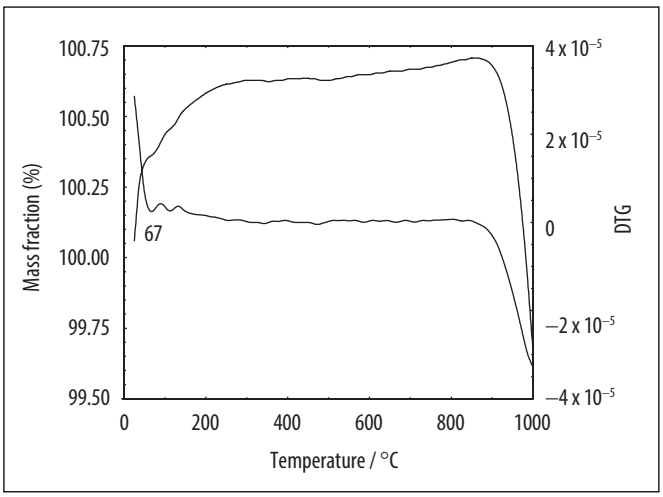

Fig. 6 **TG-DTG of commercial ZnO as standard for thermal analysis.**

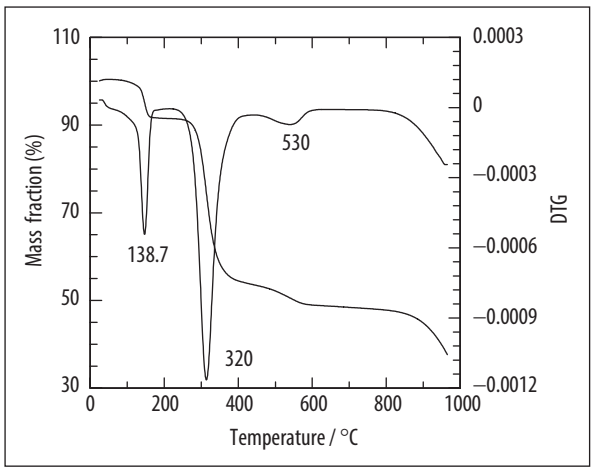

Fig. 7 **TG-DTG of ZnO-4CPA nanomaterial shows the appearance of two indo thermic bands at 138°C and 320°C.**

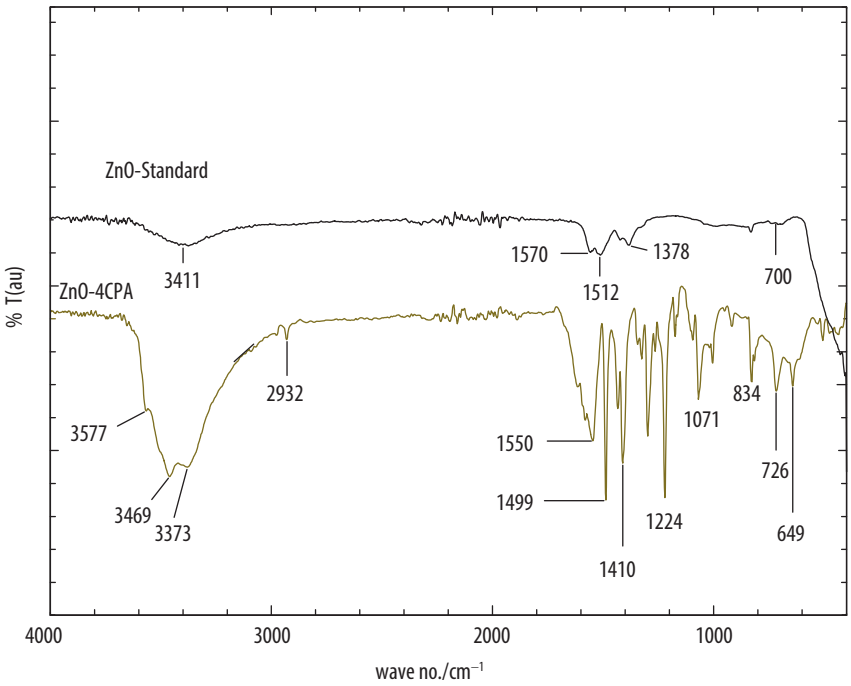

Fig. 8 **FTIR spectrums of ZnO standard and ZnO-4CPA.**

The presence of the herbicide anion in the nanohybrid can be verified by FTIR.

The broad absorption bands at 3469 cm^{-1} is due to the stretching mode of OH groups in the ZnO layer and physisorbed water. A shoulder at 3373 cm^{-1} shows the existence of hydrogen bonding between the water molecules and the ZnO layer or the anion 4CPA. The band at 1615 cm^{-1} shows a stretching band of water molecule. The band at 2930 cm^{-1} is attributed to C–H stretching vibration of the intercalated 4CPA (from $CH_2COO–$ group). Peaks at 1550 and 1326 cm^{-1} are assigned to anti symmetric and symmetric stretching vibrations of the –COO– group. The bands observed at around 1499 and 1410 cm^{-1} correspond to the C=C bond of the aromatic ring of 4CPA, herbicides.

The C–O–C anti symmetric and symmetric stretching bands appear at 1224 and 1071 cm^{-1}. Bands in the lower wave number region (i.e., 400–800 cm^{-1}) are due to M–O and M–OH bending vibration in the ZnO layers that can be seen in FTIR spectrum of Zn-4CPA and ZnO. A band observed at 829 cm^{-1} corresponding to $–CH_2$ rocking. All this indicates that it was accruals 4CPA intercalated in the ZnO interlayer which can be clearly observed at 2926 cm^{-1}.

Acknowledgment

This work was funded by ITMA-UPM, Malaysia, grant of research fellowship UPM/1.9.1. The author thanks ITMA-UPM for the study leave and scholarship. ■

References

1. Bashi AM, Hanoon JJM, Moh. Hussien Zobir, Zulkarnain Zainal. Synthesis, characterization and alteration of phenoxyherbicide-based nanocomposites resulted from mixing two herbicides with zinc oxide-layered hydroxide. Chem Mater Res. 2015;7(3):122–31.
2. Sarijo SH, Hussien MZ, Yahaya AH, Zainal Z. Effect of incoming and outgoing exchangeable anions on the release kinetics of phenoxyherbicides nanohybrids. J Hazard Mater. 2010 Oct 15;182(1–3):563–9. doi: http://dx.10.1016/j.jhazmat.2010.06.070 PMID: 20633986
3. Mane RS, Lee WJ, Lokhande CD, Cho BW, Han SH. Controlled repeated chemical growth of ZnO films for dye-sensitized solar cells. Curr Appl Phys. 2008 May;8(5): 549–53. doi: http://dx.10.1016/j.cap.2007.10.001
4. Shaheed SH, Abd. Alghanimi A, Abbas M. Bashi. Preparation of nanohybrid compounds from food preservative octyl gallate and studying some of its biological activities. Karbala Journal of Pharmaceutical Sciences 2014;7: 277–89.
5. Lee J, Easteal AJ, Pal U, Bhattacharyya D. Evolution of ZnO nanostructures in sol-gel synthesis. Curr Appl Phys. 2009 Jul;9(4):792–6. doi: http://dx.10.1016/j.cap.2008.07.018
6. Lu JJ, Lu YM, Tasi SI, Hsiung TL, Wang HP, Jang LY. Conductivity enhancement and semiconductor–metal transition in Ti-doped ZnO films. Opt Mater. 2007 July;29(11):1548–52. doi: http://dx.doi:10.1016/j.optmat.2006.08.002
7. Zhang YY, Mu J. One-pot synthesis, photoluminescence, and photocatalysis of Ag/ZnO composites. J Colloid Interface Sci. 2007 May 15;309(2):478–84. doi: http://dx.doi: 10.1016/j.jcis.2007.01.011 PMID: 17292380
8. Ghimbeu CM, Schoonman J, Lumbreras M, Siadat M. Electrostatic spray deposited zinc oxide films for gas sensor applications. Appl Surf Sci. 2007 Jul;253(18):7483–9. doi: http://dx.doi:10.1016/j.apsusc.2007.03.039
9. Lao JY, Huang JY, Wang DZ, Ren ZF. ZnO nanobridges and nanonails. Nano Lett. 2003 Feb;3(2):235–8. doi: http://dx.10.1021/nl025884u
10. Gao PX, Wang ZL. Mesoporous polyhedral cages and shells formed by textured self-assembly of ZnO nanocrystals. J Am Chem Soc. 2003 Sept;125(37):11299–305. doi: http://dx.doi.org/10.1021/ja035569p PMID: 16220952
11. Zhang Y, Jia H, Luo X, Chen X, Yu D, Wang RJ. Synthesis, microstructure, and growth mechanism of dendrite ZnO nanowires. J Phys Chem B. 2003 Aug; 107(33):8289–93. doi: http://dx.doi.org/10.1021/jp034834q
12. Zhang SC, Li XG. Preparation of ZnO particles by precipitation transformation method and its inherent formation mechanisms. Colloid Surf A: Physicochem Eng Aspects. 2003 Sept;226:35–44. doi: http://dx.doi.org/10.1016/s0927-7757(03)00383-2
13. Wang Z, Qian XF, Yin J, Zhu ZK. Large-scale fabrication of tower-like, flower-like, and tube-like zno arrays by a simple chemical solution route. Langmuir. 2004 Apr 13;20(8):3441–8. doi: http://dx.doi.org/10.1021/la036098n PMID: 1587588
14. Shen G, Bando Y, Lee CJ. Synthesis and evolution of novel hollow ZnO urchins by a simple thermal evaporation process. J Phys Chem B. 2005 Jun 2;109(21): 10578–83. doi: http://dx.doi.org/10.1021/jp051078a PMID: 16852283
15. Tong Y, Liu Y, Dong L, Zhao D, Zhang J, Lu Y, et al. Growth of ZnO nanostructures with different morphologies by using hydrothermal technique. J Phys Chem B. 2006 Oct 19;110(41):20263–7. doi: http://dx.doi.org/10.1021/jp063312i PMID: 17034205
16. Tang LQ, Zhou B, Tian YM, Bala H, Pan Y, Ren SX, et al. Preparation and surface modification of uniform ZnO nanorods via a one-step process. Colloid Surf A: Physicochem Eng Aspects. 2007 Mar;296(1–3):92–6. doi: http://dx.doi.org/10.1016/j.colsurfa.2006.09.035
17. Park NK, Lee YJ, Han GB, Ryu SO, Lee TJ, Chang CH, et al. Synthesis of various zinc oxide nanostructures with zinc acetate and activated carbon by a matrix-assisted method. Colloid Surf A: Physicochem Eng Aspects. 2008 Feb;313–314:66–71. doi: http://dx.doi.org/10.1016/j.colsurfa.2007.04.074
18. Trindade T, Pedrosa de Jesus JD, O'Brien P. Preparation of zinc oxide and zinc sulfide powders by controlled precipitation from aqueous solution. J Mater Chem. 1994;4(10):1611–7. doi: http://dx.doi.org/10.1039/jm9940401611
19. Oliveira AA, Hochepied JF, Grillon F, Berger MH. Controlled precipitation of zinc oxide particles at room temperature. Chem Mater. 2003 Aug;15(16): 3202–7. doi: http://dx.doi.org/10.1021/cm0213725

20. Chen JF, Hu Y, Zheng XS. Surfactant-assisted self-assembly growth of single-crystalline ZnO microflowers at low temperature. Colloid Surf. A: Physicochem Eng Aspects. 2008 Feb;313–314:576–80. doi: http://dx.doi.org/10.1016/j.colsurfa.2007.05.060
21. Li P, Wei Y, Liu H, Wang XK. Growth of well-defined ZnO microparticles with additives from aqueous solution. J Solid State Chem. 2005 Mar;178(3):855–60. doi: http://dx.doi.org/10.1016/j.jssc.2004.11.020
22. Xie RG, Li DS, Zhang H, Yang DR, Jiang MH, Sekiguchi T, et al. Low-temperature growth of uniform ZnO particles with controllable ellipsoidal morphologies and characteristic luminescence patterns. J Phys Chem B. 2006 Oct;110(39):19147–53. doi: http://dx.doi.org/10.1021/jp0605449
23. Shishido T, Yubuta K, Sato T, Nomura A, Ye J, Haga K. Synthesis of zinc oxide fibers from precursor bis(acetylacetonato)zinc. J All Comp. 2007 Jul; 439(1–2):227–31. doi: http://dx.doi.org/10.1016/j.jallcom.2006.05.136
24. Ban T, Sakai T, Ohya Y. Synthesis of zinc oxide crystals with different shapes from zincate aqueous solutions stabilized with triethanolamine. Cryst Res Technol. 2007 Sept;42(9):849–55. doi: http://dx.doi.org/10.1002/crat.200710960